Pro-oxidant effects of nano-TiO 2 on Chlamydomonas reinhardtii during short-term exposure

Nadia von Moos, Volodymyr Koman, Christian Santschi, Olivier Martin, Lionel Maurizi, Amarnath Jayaprakash, Paul Bowen, Vera Slaveykova

Pro-oxidant effects of nano-TiO2 on Chlamydomonas reinhardtii during short-term exposure

Nadia von Moos[1], Volodymyr B. Koman[2], Christian Santschi[2*], Olivier J.F. Martin[2], Lionel Maurizi[3], Paul Bowen[3], Vera I. Slaveykova[1]

[1] Environmental Biogeochemistry and Ecotoxicology, Earth and Environmental Science Section, Institute F.–A. Forel, University of Geneva, 10, route de Suisse, CH- 1290 Versoix, Switzerland

[2] Nanophotonics and Metrology Laboratory, Swiss Federal Institute of Technology Lausanne (EPFL), CH-1015 Lausanne, Switzerland

[3] Powder Technology Laboratory, Institute of Materials, Swiss Federal Institute of Technology Lausanne (EPFL), CH-1015 Lausanne, Switzerland

*corresponding author

e-mail: christian.santschi@epfl.ch

phone: +41 21 69 36902

KEYWORDS

nanoecotoxicity, microalgae, hydrogen peroxide, oxidative stress, oxidative damage, biosensing, cytochrome c, flow cytometry

TABLE OF CONTENTS ENTRY

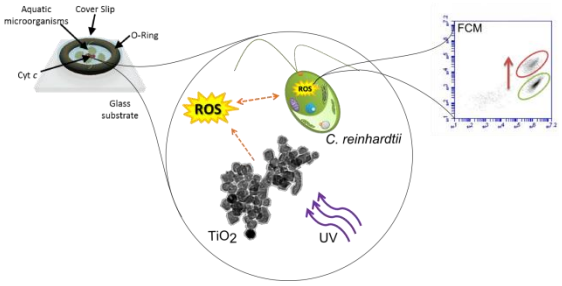

This is the first continuous quantification of abiotic and biotic nano-TiO_2 – stimulated extracellular H_2O_2 revealing how extracellular and intracellular pro-oxidant endpoints in *C. reinhardtii* differ significantly.

ABSTRACT

This study sheds light on the short-term dynamics of pro-oxidant processes related to the exposure of *C. reinhardtii* microalgae to nano-TiO_2 using a) conventional fluorescent probes for cellular pro-oxidant process and b) a novel biosensor of very high sensitivity for continuous H_2O_2 quantification. The main aims are to investigate nano-TiO_2 toxicity and the modifying factors thereof based on the paradigm of oxidative stress and to explore the utility of extracellular H_2O_2 as a potential biomarker of the observed cellular responses. This is the first study providing continuous quantitative data on abiotic and biotic nano-TiO_2-driven H_2O_2 generation to systematically investigate the link between extracellular and cellular pro-oxidant responses.

Exposure experiments of 1 h were performed in two different exposure media, with particle concentrations ranging from 10 mg L^{-1} to 200 mg L^{-1}, with and without UV pre-illumination. Abiotic and biotic extracellular H_2O_2 were continuously measured with the novel biosensor and complemented with endpoints for abiotic ROS (H_2DCF-DA), oxidative stress (CellRox Green) and damage (propidium iodide) measured by flow cytometry at the beginning and end of exposure. Results showed that extracellular and intracellular pro-oxidant processes differed significantly and that extracellular H_2O_2 cannot *per se* serve as a predictor of cellular oxidative stress or damage. The main predictors best describing the data generating processes underlying cellular responses included “exposure medium, “exposure time”, “UV treatment” as well as “exposure concentration”.

INTRODUCTION

With the increasingly pervasive use of engineered nanomaterials (ENMs) in modern society, the aquatic system has been recognized as a primary environmental entry point and sink for ENMs inevitably discharged by anthropogenic activity[1-3]. Yet, the associated inadvertent implications for the overall ecotoxicological risk remain uncertain[3-6]. The established consensus maintains that the dominant toxicity factor of inorganic ENMs lies in their ability to generate reactive oxygen species (ROS) and thereby cause oxidative stress and damage[5, 7-15]. Thus, from a nanoecotoxicological perspective seeking the elucidation of the environmental hazards of ENMs, it follows that an in depth understanding of normal and ENM-stimulated ROS production as well as antioxidant levels in aquatic organisms is required to provide risk assessors the necessary knowledge to address the following key, yet unresolved challenges of aquatic toxicology formulated by Livingstone [16] more than a decade ago: (i) identification of pro-oxidant species, (ii) design of novel toxicity assays for the detection of pro-oxidant activity, (iii) quantitative assessment of contaminant-mediated pro-oxidant processes compromising biological fitness and lastly (iv) identification of environmental and biological factors that modulate ENM-stimulated ROS generation and oxidative damage[16].

Against this background, the purpose of this research study is twofold: Firstly, it assesses the toxicity of nano-TiO_2 to the model aquatic microorganism *Chlamydomonas reinhardtii* by investigating its pro-oxidant potential and possible modifying factors thereof by well-established fluorescent probes for oxidative stress and damage. Secondly, this is the first in-depth, systematic nano-ecotoxicological study to use extracellular [H_2O_2] as a complementary endpoint in achieving the first aim, in an attempt to validate this new method based on a

cytochrome *c* biosensor, which was recently developed by a subset of the present co-authors. Unlike most other well-established approaches commonly employed in nanotoxicity testing, this novel biosensor is non-invasive and provides quantitative measurements of extracellular [H_2O_2] in real time. Given H_2O_2 is a relatively long-lived ROS, thanks to which it has a certain mobility within cells and across membranes, it is a highly suitable indicator of pro-oxidant responses in biological systems [17]. Stress-induced H_2O_2 can rapidly diffuse across the plasma membrane passively or through aquaporin channels[18, 19] and can be detected from as early as a few seconds to as long as a few days after stress application[20]. Therefore, the cytochrome *c* biosensor has been put forth a promising new method to assess and compare the pro-oxidant potential of stressors, such as nanomaterials, based on the paradigm of oxidative stress. The hypothesis to be evaluated here is the assumption that extracellular [H_2O_2] can serve as a biomarker for oxidative stress and damage in the cell originating from exposure to nano-TiO_2. In other words, we are proposing to exploit H_2O_2, a stable representative of ROS, as a possible biomarker of pro-oxidant stress. The rationale for our working hypothesis assumes that oxidative stress in cells occurs when a stressor either elevates ROS generation or weakens the antioxidant response, in which case homeostatic ROS levels are breached and H_2O_2, as the most stable ROS, is expected to be excreted by stressed cells. Thus, the present study attempts to link extracellular and cellular pro-oxidant processes in a well-described system consisting of a well-known model ENM and exposure organism.

For this purpose, the microalga *C. reinhardtii* was exposed to two series of nano-TiO_2 suspensions at nominal concentrations of 10, 50, 100 and 200 mg L^{-1}, one of which previously received a 20 min UVA illumination, in two exposure media comprising a common laboratory

testing buffer and lake Geneva water. In this way, we investigate the impact of the factors "exposure medium", "exposure concentration", "exposure time" and "UV treatment" on the pro-oxidant potential of nano-TiO_2. The pro-oxidant potential of nano-TiO_2 on the model aquatic microorganism *Chlamydomonas reinhardtii* was assessed with fluorescent probes for oxidative stress and oxidative membrane damage measured by flow cytometry (CellRox Green reagent and propidium iodide, respectively). The cellular endpoints were complemented with nano-TiO_2-induced abiotic ROS measured by H_2DCF-DA fluorescence as well as continuous measures of extracellular H_2O_2 generation measured in abiotic and biotic conditions using the cytochrome *c* biosensor.

The microalga *C. reinhardtii* employed in this study lends itself well as a model microorganism since it represents the most sensitive class of aquatic organisms to metal oxide ENMs[21] that can serve as early sentinel for potential environmental hazards in aquatic systems[22].

Nano-TiO_2 is the most abundantly produced, most widely applied and investigated ENM that assumes the role of a benchmark against which other particles can be compared[23]. Most common applications are in the fields of photovoltaics, photocatalysis and sensing but also include its use as a white pigment in paints, cosmetics, personal care products and as E-171 in food[24-27]. As a semiconductor, energies equal to or higher than its band gap around 3.2 eV (photons with wavelengths < 385 nm) generate electron-hole pairs (h_{VB}^+/e_{CB}^-) on its surface that, by reacting with surface H_2O and O_2 in aqueous media, drive the formation of various ROS, including superoxide anions ($O_2^{\bullet-}$), hydrogen peroxide (H_2O_2), free hydroxyl radicals ($OH^\bullet$) and singlet oxygen ($^1O_2$)[28-31]. With reported EC_{50} values of nano-TiO_2 for microalgae broadly varying from approximately 5 mg L^{-1} to 241 mg L^{-1} [32] its relative potency lies at the lower end of the

ENM toxicity scale. An augmented photocatalytic inhibition of algae is known[33] but it has been shown that ROS mediated nano-TiO_2 toxicity on microalgae also occurs in normal light conditions and does not significantly differ from UV treatments[34-37].

MATERIALS AND METHODS

Experimental design. Exposure experiments with algae were performed in two different exposure media and in two series of four different nano-TiO_2 concentrations (10, 50, 100 and 200 mg L^{-1}), one of which was performed with untreated particles and the other of which received a 20 min pre-illumination with long wave UV before contact with cells. Extracellular ROS was then monitored during 1 h with a novel portable oxidative stress sensor (POSS). To assess intracellular ROS levels and membrane integrity, the same exposure conditions were repeated separately and the samples stained with fluorescent probes for measurements by flow cytometry at the beginning of exposure (t = 0 h) and after 1 h (t = 1 h). All exposure conditions were replicated at least three times. All reagents (analytical grade) were purchased from Sigma Aldrich (Buchs, Switzerland), unless stated otherwise.

Algal culture. Axenic cultures of *Chlamydomonas reinhardtii* (CPCC 11) from the Canadian Phycological Culture Center (CPCC, Department of Biology, University of Waterloo, Canada) were grown in four times diluted Tris-Acetate-Phosphate (TAP×4) liquid growth medium[38] and maintained in an incubator (Infors, Bottmingen, Switzerland) at 20°C with a 24 h illumination regime (114.2 µmol phot m^{-2} s^{-1}) and constant rotary shaking (100 rpm). The culture was regularly re-inoculated in fresh growth medium and cells were harvested in mid-exponential phase. For exposure experiments, cells were gently transferred to the respective exposure

media by centrifugation (twice 805 g for 5 min, Sigma 3K10) and adjusted to a final concentration of approximately 10^6 cells mL^{-1}. All laboratory ware used for culturing was previously soaked in 5% v/v HNO_3 for at least 24h, thoroughly rinsed with MilliQ water (MilliQ Direct system, Merck Millipore, Darmstadt, Germany) and sterilized in the autoclave (Steam Sterilizer,Nüve). All crucial manipulations were performed in a sterile, laminar flow hood.

Exposure media. The exposure media included a 10^{-2} M solution of the Good's buffer 3-(N-morpholino)propanesulfonic acid (MOPS, pH = 7 ± 0.2) and Lake Geneva water (pH = 8.1 ± 0.2, physicochemical parameters provided in Table S1). Surface lake water was sampled from Lake Geneva at 46.2824° N, 6.1661° E from ca. 1.5 m depth and filter sterilized (1.2 µm with a PolyPro XL cartridge filter and 0.22 µm with an Isopore Membrane). The MOPS buffer was prepared in MilliQ water, its pH adjusted with 65% HNO_3 and sterilized by autoclave and filtration (0.22 µm Isopore Membrane, polycarbonate, Hydrophilic). The sterile exposure media were stored in the dark at 4°C.

TiO_2 handling and characterization. A stock suspension of 2 mg L^{-1} nano-TiO_2 (Degussa P25: 80% anatase, 20% rutile) was prepared in ultrapure water, sonicated in an ultrasonication bath for 10 min (Telsonic 150/300 W) and then stored at 4°C in the dark for the duration of the experiments. Primary particle properties are provided in Fig. S1. For exposure experiments, an intermediate working stock suspension was prepared by sonicating the initial stock suspension for 15 min in an ultrasonic water bath (Branson 2510) and then sampling an aliquot of 1 mL into an Eppendorf tube, which was stored in the dark at 4°C for use within 1 d. Before every experiment, this intermediate stock suspension was retrieved, sonicated in an ultrasonic bath for 5min directly before the preparation of the final, nominal exposure concentrations of 10,

50, 100 and 200 mg L^{-1} nano-TiO_2 within no more than 1 h. For all exposure conditions the number-/volume-/intensity-weighted hydrodynamic particle diameter distributions and zeta potentials were measured by dynamic light scattering (DLS) and electrophoresis with a Zetasizer Nano ZS (Malvern Instruments) at the beginning and end of exposure to cells. Hence, non-UV suspensions were measured at t = 0 and t = 60 min after suspension preparation while UV-treated suspensions at t = 20 min (initial contact with cells) and t = 80 min after suspension preparation. Samples were measured in triplicates, consisting of approximately 10 runs each. The z-average particle diameters were derived by the method of cumulants and the zeta potential was derived from the electrophoretic mobility using the Smoluchowski approximation.

UV treatment. Nano-TiO_2 suspensions received a 20 min illumination with long wave UV (300 – 420 nm = UVA) in the absorption range of nano-TiO_2 ($\lambda < 385$ nm)[39] before contact with algae. The intensity of the UV lamp (Waldmann Typ 602352 230V 50Hz 2x4W) at the sample was 60 µW cm^{-2} nm^{-1}, at the wavelength 350 nm (Fig. S2), which corresponds to an integrated intensity of 2700 µW cm^{-2} in the wavelength range 300 – 420 nm. This dose is in the range of intensities commonly occurring in natural aquatic environments[40].

Extracellular pro-oxidant processes.

Extracellular abiotic ROS. ROS in abiotic exposure conditions was qualitatively detected with the common 2',7'-Dichlorofluorescin diacetate (H_2DCF-DA, D6883-250 MG, Sigma Aldrich) assay[41, 42]. Before staining samples, the non-fluorescent dye was first dissolved in ethanol and then deacetylated by the addition of 0.01 M NaOH (pH = 7.2) in the dark, which yielded the H_2DCF molecule sensitive to oxidation. The deacetylation reaction was halted after 30 min by

the addition of 0.1 M sodium phosphate (pH = 7.2) on ice in the dark. Finally, samples were aliquoted into 96-well plates and incubated with a final concentration of 26 µM H_2DCF for 30 min in the dark, after which fluorescence was measured in a plate reader (Tecan, Infinite M200) at 485/528 ± 20 nm. For positive controls, samples were spiked with 1 mM FeSO4 (Sigma Aldrich) and 13 mM H_2O_2 (Sigma Aldrich). 3*3 replicates were prepared for every exposure condition and measured at the beginning (t = 0 h) and end of the exposure time (t = 1 h).

Quantification of extracellular abiotic and biotic peroxide. Extracellular H_2O_2 was measured with an optical, portable oxidative stress sensor (POSS), a non-invasive method recently described by Koman et al.[43] for the continuous quantification of H_2O_2 with an unprecedented limit of detection (LOD) in the nanomolar range (40 nM). The principal sensing element of the POSS consists of a ferrous heme group (Fe^{II}) embedded in the hemeprotein cytochrome *c* (cyt *c*), whose transmission spectrum at a wavelength of λ = 550 nm conspicuously evolves from a sharp peak to a broad flat dip upon oxidation to ferric iron (Fe^{III}) and the simultaneous reduction of H_2O_2 to water. This transformation can be related to the concentration of oxidizing agents, such as H_2O_2, present in in the sample. Optical measurements (in transmission mode) were performed in the reaction chamber, the core component of the POSS, consisting of an O-ring (8.0 mm * 1.0 mm, NBR Nitril, BRW) imperviously mounted onto a glass slide with grease (Dow Corning® high-vacuum silicone), forming a chamber with a volume of 60 µL to contain the sample and a cyt *c* spot, which is sealed with a cover slip. For every replicate, a new reaction chamber was prepared, filled with 80 µL of a freshly prepared sample, equipped with a freshly defrosted (fully reduced) cyt *c* spot, covered with a cover slip and excess liquid removed. Extra-cellular H_2O_2 was then continuously measured for 1 h, immediately after the initial contact of

algae with TiO_2 (max. lag time 5 min.). At the end of every 1 h measurement, reference measurements of the background scattering were performed for every sample. Cyt *c* sensing spots were previously printed onto filtration membranes, as described in Koman et al.[43] and stored in in a freezer at -20 °C until use. Nano-TiO_2 suspensions did not affect the signal of the optical sensor (Fig. S3). Calibration curves for H_2O_2 were prepared for both exposure media (Fig. S4), yielding the required values of the interaction constant *k* for the derivation of H_2O_2 concentrations according to Koman et al.[43].

Cellular pro-oxidant processes. The cellular responses oxidative stress and membrane integrity were qualitatively assessed by flow cytometry (FCM, BD Accuri C6, Accuri cytometers Inc., Michigan) equipped with a multisampler (Accuri CSampler), a 488 nm argon excitation laser, three fluorescence detectors (FL 1-3) and respective software (BD Accuri C6 1.0.264.15) for data acquisition and analysis. The fluidics rate for sampling was set to slow (14 µL min^{-1}, core size 10 µm) and run limits were set to 20,000 events per sample (gated on algae in FL3). Details on the FCM gating strategy applied for data analysis are supplied in Fig. S5 and corresponds to that previously described[44]. For every exposure condition two aliquots of 250 µL were sampled at t = 0 h and t = 1 , which were stained with fluorescent probes (Invitrogen, Life Technologies) and incubated for 30 min prior measurements. Intracellular oxidative stress was assessed with the fluorescent probe CellROX Green reagent (CRG), which was added at a final concentration of 5 µM and analyzed with the green fluorescence detector FL1 (530 ± 15 nm). Positive controls for oxidative stress were obtained by exposing algae to 0.8 mM cumene hydroperoxide for 30 min before staining with CRG. Membrane integrity was evaluated with propidium iodide (PI), added at a final concentration of 7 µM and analyzed in the orange fluorescence detector FL2 (585 ± 20

nm). Positive controls for membrane damage were obtained by exposing cells to 1 M CH_2O for 30 min before adding PI.

Statistical analysis. Graphs were prepared with Origin Pro 8 and R version 3.1.3 "Smooth Sidewalk". For statistical analysis, FCM data was log-transformed and two obviously aberrant outliers were removed. To analyze the underlying data generating factors of the discrete data sets obtained for abiotic ROS (measured by H_2DCF-DA), oxidative stress (CellRox Green) and membrane integrity (propidium iodide) a linear regression model was fit with R, containing the main predictors "exposure medium", "exposure time", "exposure concentration" and "UV treatment" (medium + time + concentration + UV) and all their interactions (medium:time, medium:concentration etc.). Model selection was performed by the BIC (simple model) and AIC (complex, more predictive model, see ESI 2.1). Since abiotic ROS measurements and cellular endpoints have different units (fluorescence in a.u. and % affected cells, respectively), statistical analyses were performed separately. All R output tables and residual analyses are provided in the Electronic Supplementary Information (ESI, Tables S2 – S11, Figs. S10 and S11).

RESULTS AND DISCUSSION

1. Particle stability in exposure conditions

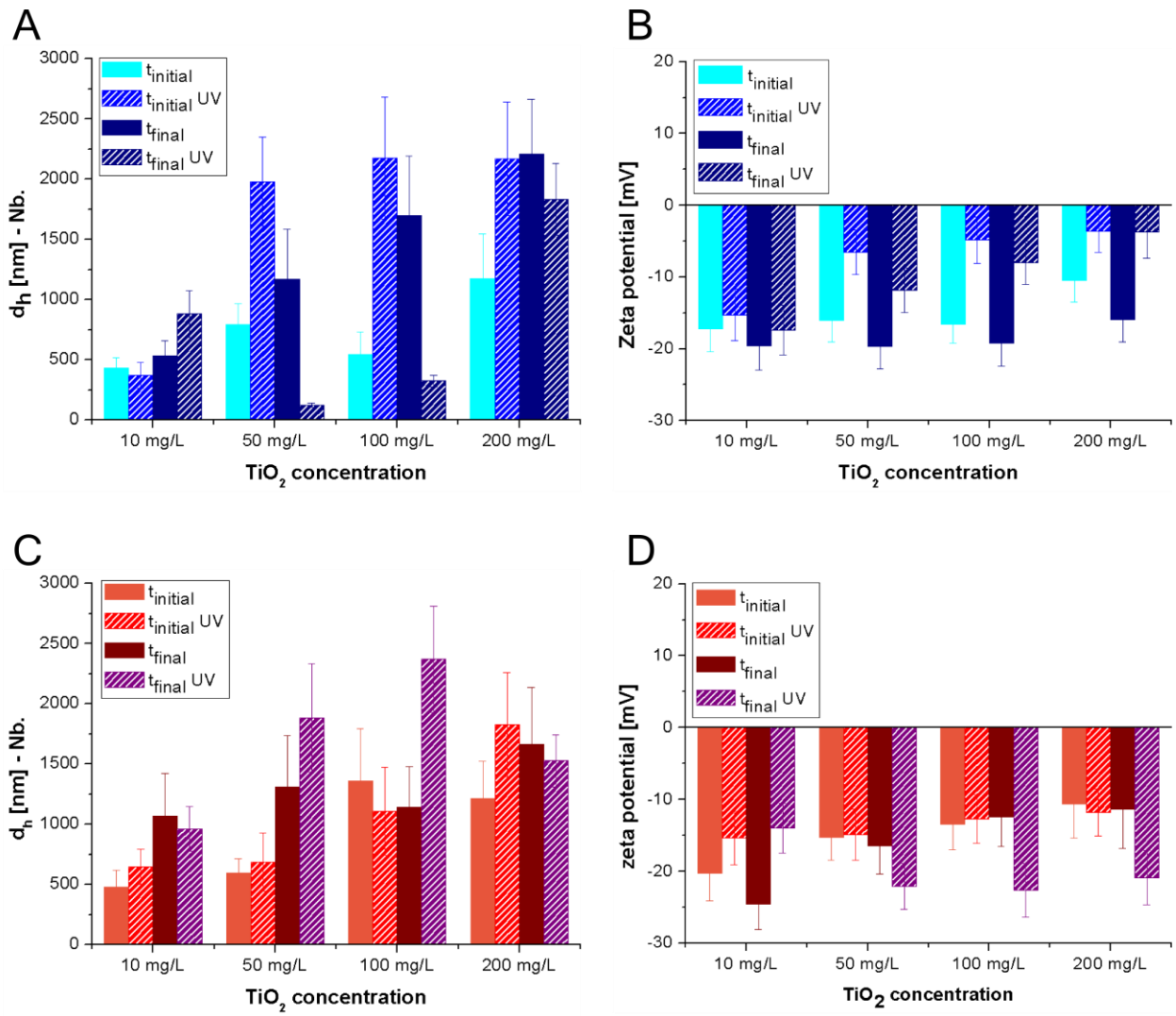

Figure 1. Mean and standard deviation of number-weighted hydrodynamic diameters (d_h – Nb.) in [nm] (A, C) and zeta potentials in [mV] (B, D) of different nano-TiO_2 concentrations in lake water (A, B) and MOPS (C, D) at the beginning ($t_{initial}$) and end (t_{final}) of the 1 h exposure. Diameters for untreated samples correspond to times $t_{initial}$ = 0 min and t_{final} = 60 min (after the preparation of the suspension). Diameters of UV pre-treated samples correspond to times $t_{initial}$ *UV* = 20 min and t_{final} *UV* = 80 min after suspension preparation.

Hydrodynamic diameter (d_h). Nano-TiO_2 suspensions are heavily agglomerated in both exposure media, with number-weighted d_h roughly ranging between 200 nm and 2500 nm (Fig.

1, A and C). Volume- and intensity–weighted d_h are provided in the ESI (Fig. S6) and showed similar trends (Fig. S7, A and B). The hydrodynamic diameters detected are at the extreme limit of the DLS method and the measured sizes will be unreliable but the trends seem to be consistent. General trends of untreated particles showed that d_h increased with nano-TiO_2 concentration (d_h (10 mg L^{-1}) < d_h (200 mg L^{-1})) and time (d_h ($t_{initial}$) < d_h (t_{final})) in both media (Fig. 1, Fig. S7, C - F). D_h at $t_{initial}$ were largely slightly higher in MOPS than in lake water.

These findings are in agreement with earlier observations of nano-TiO_2 forming agglomerates of several hundred nanometers to several micrometers in diameter within minutes at environmentally relevant pH, ionic strengths and DOM[45, 46]. A comprehensive study investigating the behavior of nano-TiO_2 in natural matrices at the same concentrations employed here found very low sedimentation rates in freshwater suggesting ecotoxicologically relevant residence times of agglomerated nano-TiO_2 for aquatic organisms in the water column[47].

The trends for UV pre-illuminated suspensions in lake water showed d_h ($t_{initial}$ *UV*) > d_h (t_{final} *UV*) in 50 mg L^{-1} , 100 mg L^{-1} and 200 mg L^{-1}suspensions. This relation was inverse in 10 mg L^{-1} suspensions. In the MOPS buffer d_h ($t_{initial}$ *UV*) < d_h (t_{final} *UV*), except in the 200 mg L^{-1} suspension (Fig. 1, A and C).

All in all, particles in the present exposure system were no longer in the nanometer range but much ranger formed colloid-sized agglomerates in the micrometer size range. For comparison, *C. reinhardtii* cells have diameters around 5 – 10 µm, and are thus roughly equal to one order of magnitude larger than agglomerates observed here.

Zeta potential. The zeta potential values of untreated particles in lake water lay between -20 mV and -15 mV and decreased slightly with increasing particle concentrations (Fig. S7, E and F), reaching values around -10 mV in the 200 mg L^{-1} suspension. This could contribute to the comparably smaller d_h (i.e. greater suspension stabilities) observed in the lower concentrations. The values were largely comparable at $t_{initial}$ and t_{final}. UV treated particles in lake water were generally less negative with values ranging from -3 mV to –15 mV and values at t_{final} *UV* were either equal or more negative than at $t_{initial}$ *UV*, which matches the elevated d_h observed at $t_{initial}$ *UV* and also the decrease in d_h observed at t_{final} *UV* (Fig. 1, A). Likewise, the zeta potential values in the MOPS buffer roughly varied between -20 mV and -10 mV but were overall nearer – 10 mV and thus slightly less negative than particles in lake water, likely due to the absence of DOM. Previous findings have also shown that charge repulsion between particles and HS occurred in conditions where pH > isoelectric point[48], which may explain the overall similarity of d_h in the two media observed here. In the MOPS buffer zeta potentials of untreated particles remained more or less the same at the beginning and end of exposure. The zeta potential of UV-treated particles at $t_{initial}$ *UV* were generally either equal or more negative than at t_{final} *UV* (Fig. 1D) but, rather puzzlingly, d_h(t_{final} *UV*) were greater than d_h($t_{initial}$ *UV*).

2. Extracellular pro-oxidant processes

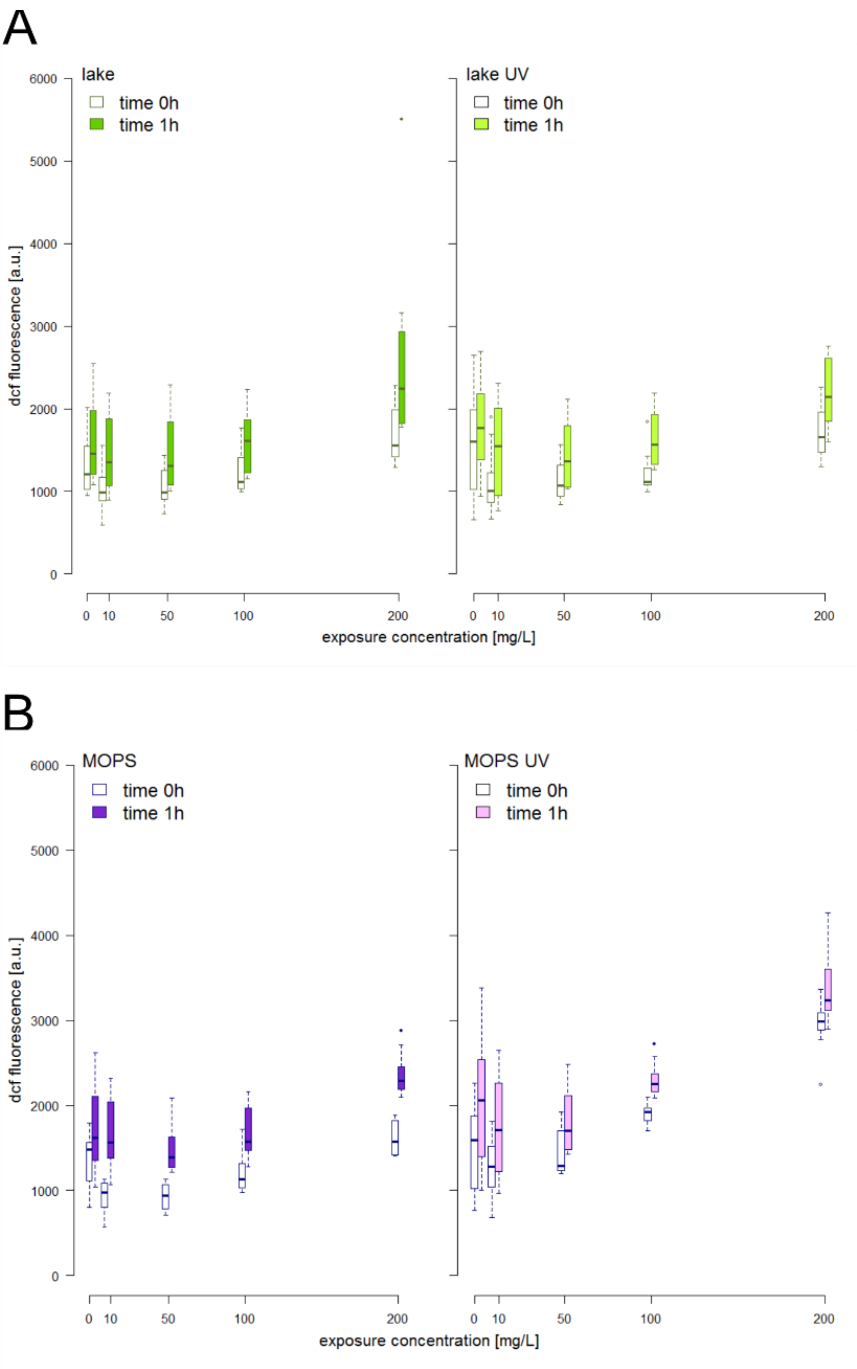

Figure 2. Abiotic ROS measured as DCF fluorescence after t = 0 h and t = 1 h in lake (A) and MOPS (B) at different nano-TiO_2 concentrations with and without 20 min UVA pre-illumination of nano-TiO_2 suspensions. Box-whisker plots show median of at least triplicate measurements and the respective quantiles with whiskers indicating minima and maxima within 1.5 of the interquantile range.

Abiotic ROS. In both media elevated, above control median levels of ROS, as measured by H_2DCF-DA, were only observed at 200 mg L^{-1} nano-TiO_2 (Fig. 2A and 2B). UV treatment of nano-TiO_2 suspensions did not significantly affect results in lake water, but in the MOPS buffer produced higher median levels of abiotic ROS, most pronounced at 100 and 200 mg L^{-1} nano-TiO_2 (t = 0 h and t = 1 h, Fig. 2B).

Abiotic and extracellular biotic peroxide in lake water. In contrast to the measured abiotic ROS, the peroxide measurements obtained by POSS indicate a nano-TiO_2 concentration dependent level of abiotic peroxide in lake water (Fig. 3A) and overall increased abiotic peroxide levels in UV treated nano-TiO_2 suspensions (Fig. 3B). Much like abiotic ROS measured by H_2DCF-DA, the highest level of peroxide was observed at 200 mg L^{-1} nano-TiO_2 (Fig. 3A). UV treatments produced c_{H2O2} peaks immediately at t = 0, which exponentially decreased within the first 10 to 20 min (Fig. 3B) but did not show any concentration dependent trends. The respective decay rate constants are provided in Table 1 and plotted in Figure S9.

In biotic settings, the algae only treatment as well as algae exposed to 10 mg L^{-1} nano-TiO_2 yielded the highest c_{H2O2} values around 50 – 60 nM, all other conditions produced lower concentrations of peroxide (Fig. 3C). The combination of UV pre-treated nano-TiO_2 suspensions with algae (Fig. 3D) did not reproduce the characteristic peroxide peak previously observed in the abiotic UV treatment (Fig. 3B) and consistently yielded lower peroxide levels than in biotic conditions (Fig. 3C).

H_2O_2 has a lifetime of up to 10 h (or longer) in the environment (pH = 7)[49, 50] that may explain the steady concentrations observed during 1 h, which are well in the range of those typically occurring in natural surface waters ranging from 10 pM to 100 nM[49].

These observations lead us to the following interim conclusions: i) In lake water the POSS method is more sensitive to peroxide than the H_2DCF-DA stain to peroxide and/or ROS, ii) in lake water the presence of algae can either increase (10 and 50 mg L^{-1} treatments) or decrease extracellular peroxide levels (100 and 200 mg L^{-1} treatments) observed in abiotic conditions, iii) *C. reinhardtii* do not release excess peroxide above the baseline of negative controls when exposed to nano-TiO_2 (Fig. 3C) and finally iv) algae exposed to UV activated nano-TiO_2 (Fig. 3D) quench the excess peroxide peak observed in abiotic UV treatments (Fig. 3B).

Abiotic and extracellular biotic peroxide in MOPS buffer. Unlike in the lake water system, c_{H2O2} in the MOPS buffer peaked at t = 0 h in all concentrations, in both treatments, and exponentially decreased within the first 10 – 20 minutes to relatively stable lower values hovering around or below the LOD (Fig. 4A-D). The corresponding exponential decay rates are provided in Table 1 and plotted in Figure S9.

Overall, peroxide levels increased in the presence of *C. reinhardtii* and even surpassed the baseline level of the negative control in exposures to 50, 100 and 200 mg L^{-1} nano-TiO_2 (Fig. 4C). This was most evident in the 200 mg L^{-1} nano-TiO_2 exposure where an additional surge in c_{H2O2} was observed beginning at t = 10 min and peaking at t = 60 min, which did not occur in any other treatment (Fig. 4C).

In MOPS the UV pre-irradiation of nano-TiO_2 actually increased initial biotic c_{H2O2} peak values but on the long run lead to lower biotic peroxide levels compared to non-UV treatments, except in the 10 mg L^{-1} treatment showing higher c_{H2O2} values than the negative control (Fig. 4D).

The initial peak in c_{H2O2} was observed in all conditions without exception and presumably resulted from the generation of h_{VB}^{+}/e_{CB}^{-} on particle surfaces through sonication prior exposure

and photocatalytic reactions with H_2O and O_2 [51]. The generation of ROS in aqueous solutions through sonication and acoustic cavitation effects is also a well-known phenomenon[17]. There are several possible pathways for the subsequent extinction of H_2O_2. For example, measured c_{H2O2} levels and the respective decay rate constants obtained in abiotic conditions were inversely related to particle concentrations in both media (Table 1, Fig. S9), indicating that total particle surface area is an important factor governing ROS generation and quenching. Therefore, nano-TiO_2 probably behaved as both a source and sink of c_{H2O2} by sonication/UV-generated reactive h_{VB}^+/e_{CB}^- at the particle surface reacting both with H_2O/O_2 and ensuing ROS. Since the dynamics of c_{H2O2} decay were identical in distilled water it can be inferred that the reaction of H_2O_2 with nano-TiO_2 was presumably the dominant decay mechanism.

These observations lead us to the following tentative conclusions i) in the MOPS buffer sonication of nano-TiO_2 may explain the initial peroxide peak observed in nearly all MOPS treatments, which unlike lake water does not possess ROS quenching species such as DOM, ii) *C. reinhardtii* slightly elevate peroxide levels when exposed to nano-TiO_2 in MOPS, suggesting a biological contribution either from redox reactions at the cell surface or from intracellular ROS/peroxide diffusing out.

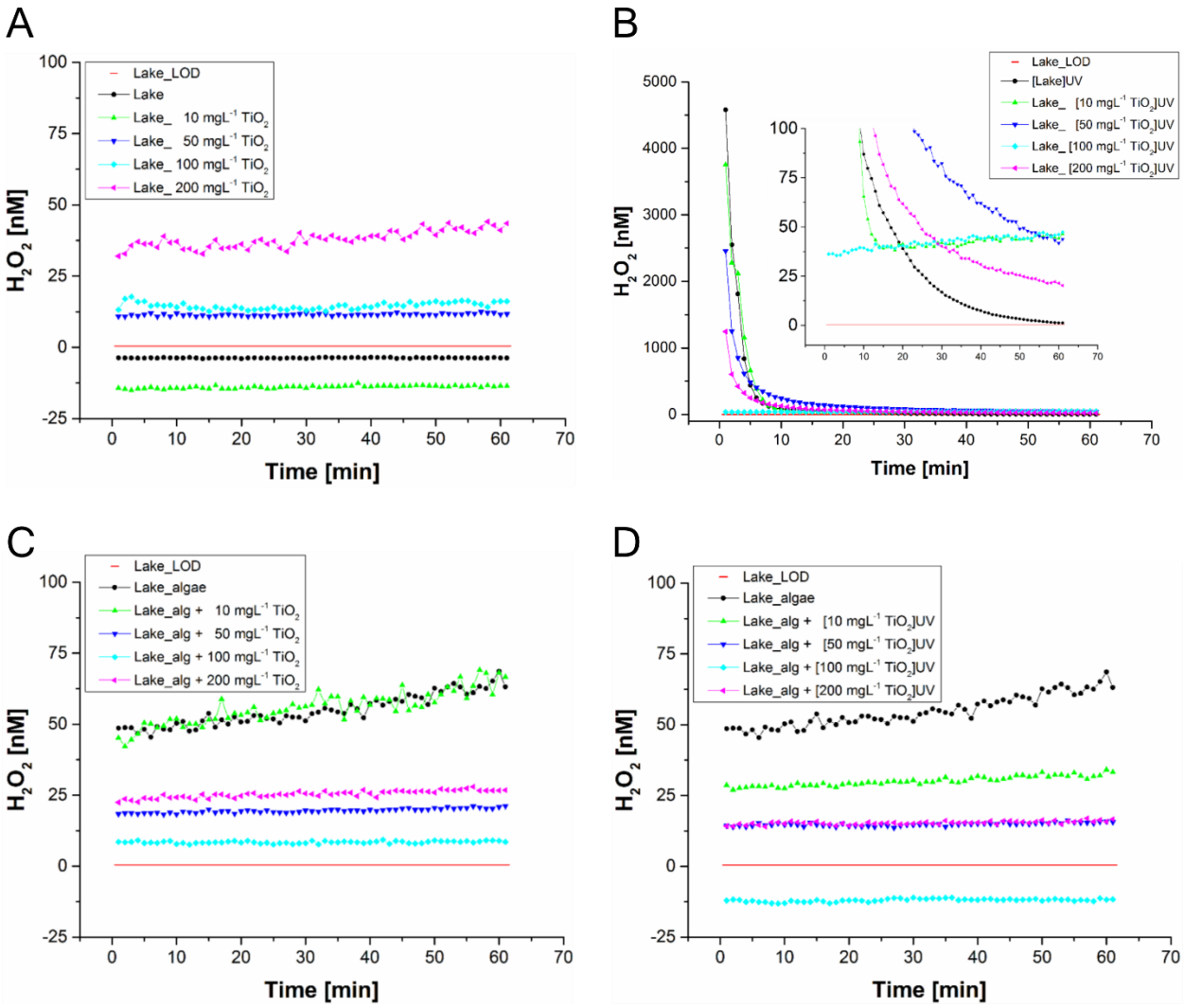

Figure 3. Average extracellular H_2O_2 [nM] (c_{H2O2}) (of at least triplicate measurements) produced during 60 min by four nano-TiO_2 concentrations with (B, D) and without UV pretreatment (A, C) in abiotic (A, B) and biotic (C, D) conditions in lake water: nano-TiO_2 only (A), nano-TiO_2 after 20 min UV pre-treatment (B), algae exposed to nano-TiO_2 (C) and algae exposed to UV pre-treated nano-TiO_2 (D). The horizontal red line represents the LOD and the inset in (B) shows a close-up of the 0 – 100 nM concentration range.

Table 1. Decay rate constants (b [min^{-1}] extracted from fitting the function Ae^{-bt} to c_{H2O2} (t)) in the initial exponential phase to extracellular H_2O_2 measured by POSS, as plotted in Fig. 3 and Fig. 4. Also plotted in Figure S9. NA = not available.

	without TiO_2		10 mgL^{-1} TiO_2		50 mgL^{-1} TiO_2		100 mgL^{-1} TiO_2		200 mgL^{-1} TiO_2	
	no UV	**UV**	**no UV**	**UV**	**no UV**	**UV**	**no UV**	**UV**	**no UV**	**UV**
lake water										
abiotic ROS	NA	0.203	NA	**0.206**	NA	0.173	NA	NA	NA	0.167
biotic ROS	NA	NA	NA	NA	NA	NA	NA	NA	NA	NA
MOPS buffer										
abiotic ROS	NA	0.06	0.259	NA	0.143	**0.420**	0.094	0.222	0.076	0.275
biotic ROS	0.042	NA	NA	0.261	0.108	0.175	0.139	0.189	0.234	**0.275**

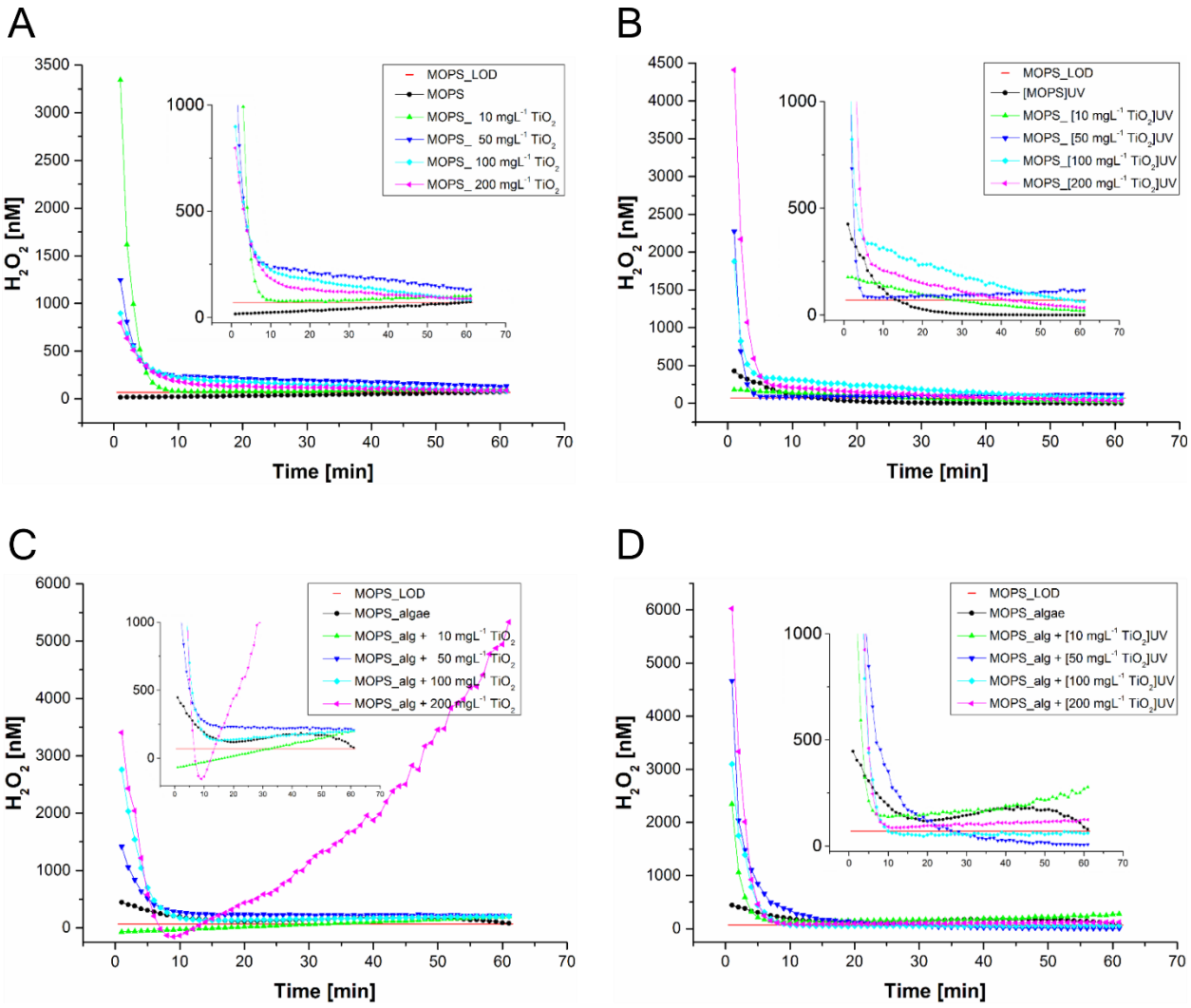

Figure 4. Average extracellular H_2O_2 [nM] (c_{H2O2}) (of at least triplicate measurements) produced during 60 min by four nano-TiO_2 concentrations with (B, D) and without UV pre-treatment (A, C) in abiotic (A, B) and biotic (C, D) conditions in the MOPS buffer: nano-TiO_2 only (A), nano-TiO_2 after 20 min UV pre-treatment (B), algae exposed to nano-TiO_2 (C) and algae exposed to UV pre-treated nano-TiO_2 (D). The horizontal red line represents the LOD and insets depict enlargements of the respective 0 – 1000 nM concentration range.

3. Cellular pro-oxidant processes: oxidative stress and damage

Oxidative stress in lake water. In lake water exposures the proportion of cells affected by oxidative stress did not exceed 5 % (Fig. 5A, Table S2) but intracellular ROS levels showed a concentration dependent increase after 1 h of exposure in both treatments, with highest responses obtained for algae exposed to 100 and 200 mg L^{-1} nano-TiO_2. UV treatments only minutely enhanced median intracellular ROS levels in lake water, leading to slightly higher values at t = 1 h in [50 mg L^{-1}]UV and [100 mg L^{-1}]UV treatments (Fig. 5A, Table S2). Controls and 10 mg L^{-1} nano-TiO_2 exposures produced comparable responses in both treatments (Fig. 5A).

Oxidative stress in MOPS.

In the MOPS buffer, although high extracellular c_{H2O2} were measured in biotic conditions, no effects on intracellular ROS levels were observed in both treatments (Fig. 5A, Table S3). A marked increase in the proportion of cells with elevated intracellular ROS was observed in all conditions after 1 h, including the controls, suggesting that the MOPS medium may have acted as a stressor itself (Fig. 5A). The pre-irradiation of nano-TiO_2 with UV slightly reduced median intracellular ROS responses at all concentrations in the MOPS buffer.

Membrane integrity in lake water. Membrane damage predominantly occurred in lake water (Fig. 5B, Table S8 and S9) and the proportion of affected cells was more than one order of magnitude higher than in MOPS. In lake water, membrane impairment was considerably elevated in cells exposed to 100 and 200 mgL^{-1} untreated nano-TiO_2 for 1 h reaching 12 % and 19 % affected cells, respectively, compared to ca. 8 % in controls. There was no difference in membrane damage between controls and cells exposed to 10 mg L^{-1} and 50 mg L^{-1} nano-TiO_2

(Fig. 5B, Table S8). UV pre-treated nano-TiO_2 did not greatly affect responses, but rather even decreased the proportion of affected cells (Fig. 5B).

Membrane integrity in MOPS. In MOPS the effects of nano-TiO_2 on the membrane integrity of *C. reinhardtii* were altogether negligible (< 1 %, Fig. 5B, Table S7). No differences in membrane damage were observed between control and exposed cells but opposed to results obtained for intracellular ROS, the membrane integrity of controls was not affected by the MOPS medium itself.

Overall, cellular responses were higher in lake water exposures, which is in agreement with earlier results showing a heightened toxicity of nano-TiO_2 on developing zebrafish in the presence of humic acid [52] but contradicts others showing a mitigation of nano-TiO_2-induced pro-oxidant effects on the alga *Chlorella sp.* through increased electrosteric repulsion[53].

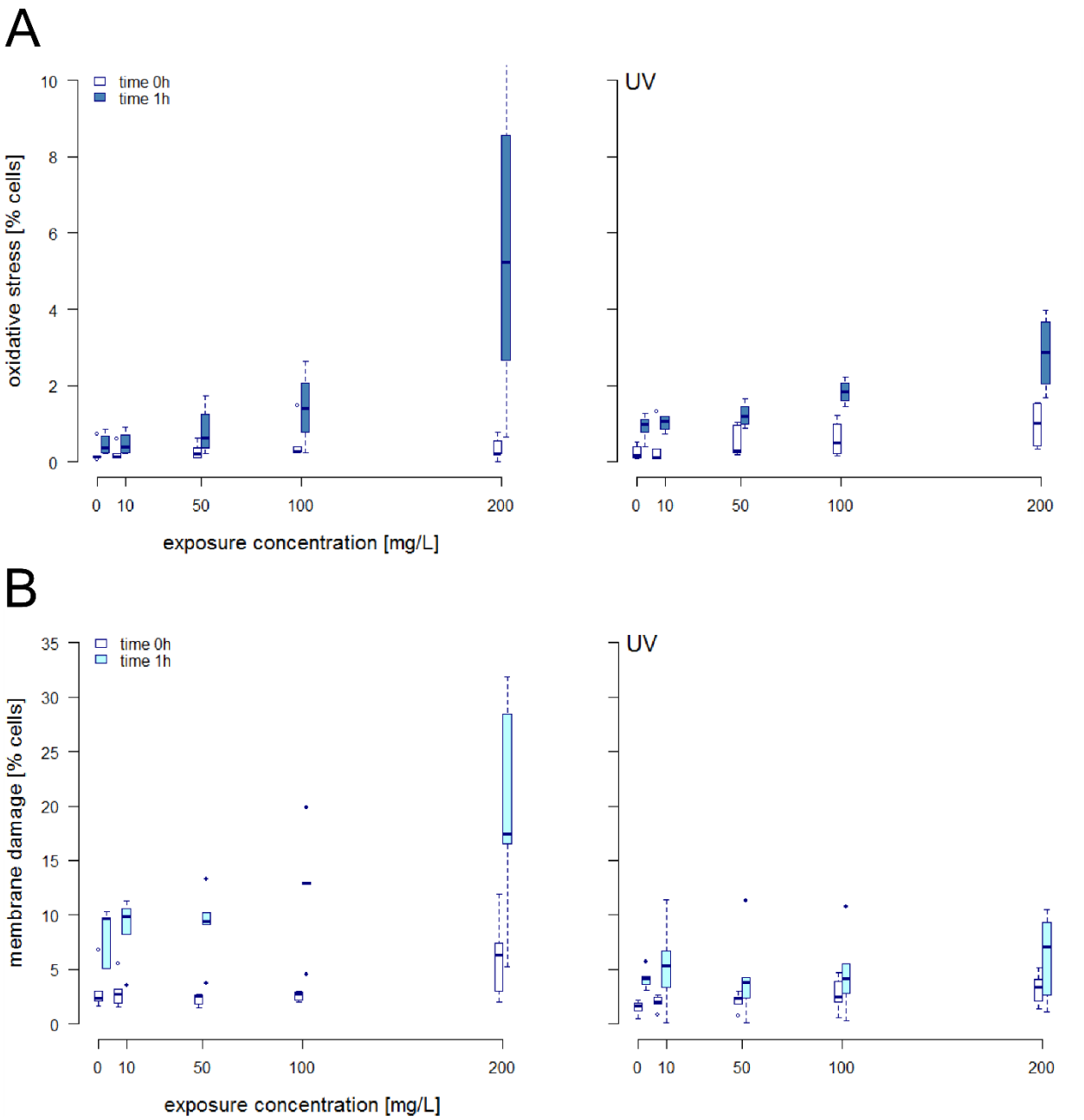

Figure 5. Box-whisker plots showing the median, quantiles and S.D. (of at least triplicates) of intracellular ROS (A) and membrane damage (B) in [% affected cells] of the total number of cells exposed to 0, 10, 50, 100 and 200 mg L^{-1} nano-TiO_2 concentrations without (left plot) and with UV pre-treatment (right plot) in lake water at the beginning (t = 0 h) and end of exposure (t = 1 h).

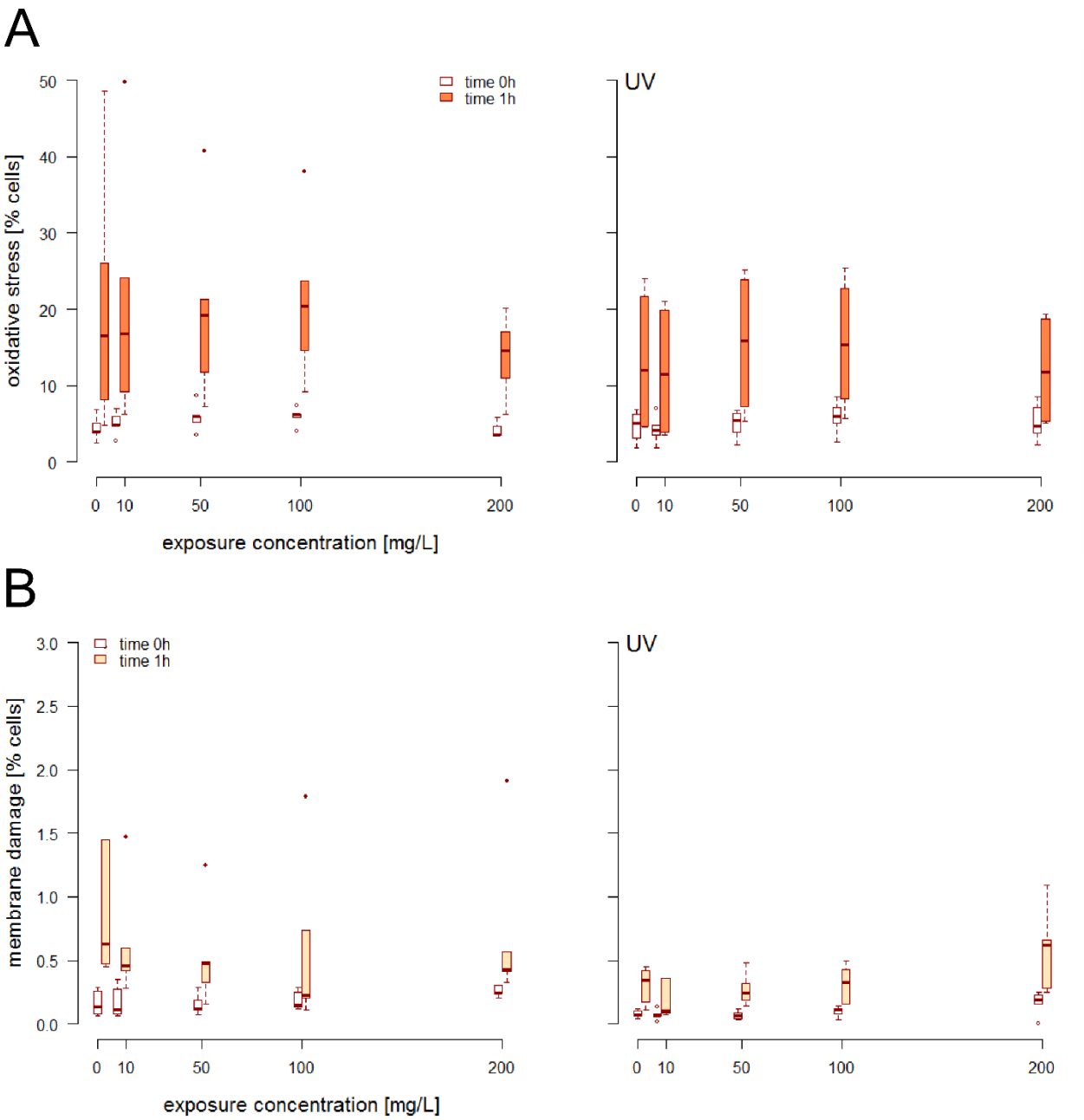

Figure 6. Box-whisker plots showing the median, quantiles and S.D. (of at least triplicates) of intracellular ROS (A) and membrane damage (B) in [% affected cells] of total number of exposed cells to different TiO_2 concentrations without (left plot) and with UV pre-treatment (right plot) in the MOPS buffer at the beginning (t = 0 h) and end of exposure (t = 1 h).

4. Main predictors of pro-oxidant processes.

For all three endpoints, all main effects including several interaction terms were retained in the more complex AIC selected models. In the simpler BIC models (Tables S2, S6 and S10) the main effect “exposure concentration” was not retained in the models fitted to the cellular endpoints (Table 2).

For the ROS related endpoints (H_2DCF-DA and CellRox Green) the AIC models suggest a significant effect of exposure concentration, as well as interaction between exposure concentration and exposure medium. More generalized, this finding implies that pro-oxidant processes of varying nano-TiO_2 concentrations will differ as a function of the ambient medium. On the other hand, the effect of varying nano-TiO_2 concentrations on membrane damage is simply an additive factor, independent of the respective levels of all the other factors while the impact of the medium will be influenced by the exposure time and UV treatment and vice versa. More generalized, this implies that the medium itself plays a significant role in membrane integrity.

Furthermore, we can infer from the fitted models that the effect of UV treatment on all endpoints considered will significantly depend on the exposure medium.

These relationships can also be visually related to the data presented above (Figs. 2, 5 and 6).

Table 2. Summary of linear models fitted to data for abiotic ROS and cellular endpoints of stress (Tables S2-S11, Figs. S10 and S11).

Endpoint: abiotic ROS	
BIC model:	`medium + time + UV + conc + medium:UV + medium:conc + UV:conc + medium:UV:conc`
AIC model:	`medium + time + UV + conc + medium:UV + time:UV + medium:conc + UV:conc + medium:UV:conc`
Endpoint: oxidative stress	
BIC model:	`medium + time + UV + medium:UV`
AIC model:	`medium + time + UV + conc + medium:UV + medium:conc`
Endpoint: membrane damage	
BIC model:	`medium + time + UV`
AIC model:	`medium + time + UV + conc + medium:UV + time:UV + medium:time + medium:time:UV`

5. Linking extracellular processes to cellular pro-oxidant processes.

Overall, the cH_2O_2 results obtained by POSS provide evidence that (i) irrespective of the medium, agglomerated nano-TiO_2 in the micrometer size range produced abiotic H_2O_2 in biologically relevant media, which is enhanced by UV irradiation, (ii) the generation of H_2O_2 and/or the measured cH_2O_2 is a dynamic process and is modified by the ambient medium as well as the nano-TiO_2 concentration and lastly (iii) the presence of cells either decreased or increased total c_{H2O2} measured in equivalent cell-free conditions. In view of our results showing both an additive and quenching effect of c_{H2O2} in the presence of algae, we will now examine cellular responses in an attempt to link extracellular processes with pro-oxidant processes at the cellular level.

The exposure of algae to nano-TiO_2 in lake water did not produce cH_2O_2 above the level of unexposed controls. Nonetheless, the presence of cells reduced cH_2O_2 levels obtained for 100 and 200 mg L^{-1} exposures but increased those of 10 and 50 mg L^{-1} exposures with respect to the corresponding abiotic values (Fig. 3). On the other hand, exposure of algae to 50, 100 and 200

mg L^{-1} nano-TiO_2 in MOPS produced higher cH_2O_2 levels than in the respective controls. After t = 1 h the 10 mg L^{-1} exposure also surpassed the negative control. Similarly, exposure to UV treated nano-TiO_2 surpassed the baseline cH_2O_2 levels of controls in the initial 10 – 20 min of exposure with the 10 mg L^{-1} exposure remaining high until the end of exposure at t = 1 h (Fig. 4). Based on these observations and assuming the initially stated working hypothesis whereby peroxide may serve as a marker for oxidative stress in cells as true, we would thus anticipate i) no intracellular oxidative stress and damage in lake water treatments (Fig. 5) and ii) elevated intracellular ROS levels and membrane damage in cells exposed in MOPS (Fig. 6).

In fact, quite the opposite was observed. Oxidative stress (albeit low values) and membrane damage (up to 15 % cells affected) were primarily observed in lake water exposures while there was no evidence of elevated cellular pro-oxidant stress in either controls or treatments conducted in MOPS. From the point of view of the original working hypothesis from which we departed these observations are not immediately obvious but there are several plausible explanatory hypotheses we can infer. However, the present experimental setup does not provide sufficient resolution as to support one hypothesis over the other.

Lake water. Oxidative stress and membrane damage in lake water treatments were highest in exposures to 100 and 200 mg L^{-1} nano-TiO_2. At the same time biotic c_{H2O2} in 100 and 200 mg L^{-1} exposures decreased compared to identical abiotic conditions while biotic c_{H2O2} in exposures to 10 and 50 mg L^{-1} increased. UV treatment produced abiotic c_{H2O2} peaks at the beginning of exposure time which disappeared in the identical biotic settings. Oxidative stress only marginally increased in UV treatments and biotic c_{H2O2} remained markedly below the level in unexposed controls.

By inference we may conclude that oxidative stress and membrane damage was likely mediated by free extracellular H_2O_2 reacting at the cell surface. H_2O_2 can directly oxidize DNA, lipids, -SH groups and can inactivate enzymes [54]. Although H_2O_2 is a rather weak oxidizing agent for biomolecules and particularly lipids [20], it readily reacts with e^-_{CB}, $O_2^{\bullet-}$ or, in the presence of transition metal ions, engages in Fenton reactions leading to the formation of the highly reactive, short-lived, indiscriminate oxidant $OH^\bullet$ [49, 51]. DOM is another source of hydroxyl radical formation [49, 54]. The likely presence of trace amounts of metals in lake water samples in combination with DOM/nano-TiO_2–generated H_2O_2 may have facilitated the generation of the more reactive $OH^\bullet$ that more rapidly and readily oxidizes biomolecules such as lipids and thereby escaped detection by cyt *c*, leading to relatively low measured c_{H2O2} and higher levels of oxidative stress and membrane damage in exposed cells. In extension, UV treatment induced slightly elevated oxidative stress levels (except at 200 mg L^{-1}) as a consequence of extra $OH^\bullet$ emerging from UV generated c_{H2O2}. The ecotoxicological implications of Haber-Weiss reactions have previously been evoked[55] and demonstrated that environmentally relevant concentrations of redox and nonredox active metals enhanced intracellular ROS in *C. reinhardtii*, without affecting algal photosynthesis.

Alternatively, DOM is a known ROS scavenger. It is quite feasible that DOM competed with the cyt *c* for H_2O_2 possibly emanating from stressed cells and thereby buffered extracellular c_{H2O2}. Finally, the observed responses may have also ensued from direct physical interactions between nano-TiO_2 and cells. It is well-known that increased ROS and oxidative damage may not only result from a contaminant's direct pro-oxidant effects. Rather, interactions with a

contaminant can lead to some physical injury, which in turn can lead to excess ROS or ROS-generating species[16].

MOPS. Much in contrast, in the MOPS buffer significant concentrations of c_{H2O2} were measured in the presence of nano-TiO_2 both in abiotic and biotic exposure conditions, with no significant cellular effects whatsoever. Hence, results suggest that neither direct particle - cell interactions nor freely diffusing extracellular H_2O_2 adversely affected *C. reinhardtii*. In the biotic setting, initial and final c_{H2O2} were higher compared to equivalent abiotic conditions for all concentrations but the 10 mg L^{-1} nano-TiO_2 treatment. This implies that algae contributed to the net measured c_{H2O2}, either through the leaching of intracellular ROS or through reactions of H_2O_2 with the cell surface. Both these hypotheses seem feasible in view of the above observations:

If we consider that H_2O_2 is a relatively weak oxidizer[20, 49] (particularly in absence of transition metal ions that would enable the formation of the more reactive hydroxyl radical) and both intracellular ROS and membrane integrity were not significantly elevated in exposed cells at the beginning of exposure, the excretion of H_2O_2 by cells is a plausible explanation for the net increase in c_{H2O2} at the beginning of exposure. It is known from plants for example that extracellular H_2O_2 concentrations can increase in response to abiotic stressors and environmental pollutants such as metals, pesticides and salt during what is known as the oxidative burst.

On the other hand, previous findings showed an accumulation of nano-TiO_2 on the cell surface of microalgae exposed to similar nano-TiO_2 concentrations[37, 56-58] and postulated that oxidation occurred through surface-bound ROS which are not free to diffuse into the cell[59], which is the

second possible explanation for the observed increase in c_{H2O2} in biotic conditions. It is widely acknowledged that proximity or direct contact is a prerequisite for ENP toxicity, without which direct oxidation of cellular components or physical disruption of cell walls and membranes would not occur[30, 59, 60]. However, assuming this scenario, one would expect oxidative stress or oxidative damage in exposed cells, which was not the case. The absence of transition metals in the MOPS buffer may explain why membrane integrity did not degenerate as fast, despite the elevated levels of c_{H2O2} both in UV pre-treated and untreated nano-TiO_2 suspensions. Therefore, c_{H2O2} excretion by cells seems more plausible.

UV treatment. The pre-illumination of nano-TiO_2 suspensions considerably affected abiotic c_{H2O2} in both media and rather unexpectedly only marginally enhanced oxidative stress in lake water exposures, which is in agreement with earlier findings showing no UV enhanced toxicity of nano-TiO_2 on microalgae[34]. The pre-illumination of lake water itself generated the highest concentration of ROS, which can result from the absorption of UV by DOM and its subsequent photolysis[50, 61]. An initial peak in c_{H2O2} was observed in all conditions in MOPS but only in the abiotic UV treatments in lake. DOM is also known to scavenge c_{H2O2}, which may explain the fairly steady c_{H2O2} over time compared to concentrations measured in MOPS. Thus, the additional energy input by UV may have provided an additional source of H_2O_2 generation through DOM photolysis, which could no longer be scavenged by DOM and thus produced the initial c_{H2O2} peaks in the UV treatments. The elevated c_{H2O2} measured in cell-free UV pre-treated nano-TiO_2 suspensions in lake water disappeared in the presence of cells, which supports the above hypothesis by which free extracellular H_2O_2 react with exposed algae (and/or possibly transform into highly reactive hydroxyl radicals via Fenton reactions). Plant cells are actually

known to consume extracellular H_2O_2 concentrations as high as 10 mM in less than 10 min, as demonstrated by its rapid depletion by *Arabidopsis thaliana* within 8 – 10 min[62, 63]. The proportion of cells with oxidative stress was higher than in non-UV treatments and increased in a concentration dependent manner, except in the [200 mg L^{-1}]UV exposure. Bearing the biotic, non-UV responses in mind, this suggests an additive pro-oxidant effect of H_2O_2 and thus supports the hypothesis of extracellular H_2O_2 reacting with cells in lake water as primary cause over direct cell-particle interactions. This contradicts previous findings reporting that artificial UV irradiance of two temperate German lakes with moderate DOM levels (dissolved organic carbon (DOC) = 15 mg L^{-1}) generated H_2O_2 concentrations in the range of 150 – 360 nM, which did not adversely affect the three microalgae *Chlorella sp.*, *Desmodesmus subspicatus* and *Scenedesmus obliquus* (measured by delayed fluorescence kinetics)[50]. Despite lower DOM levels in Lake Geneva water samples (DOC = ca. 1 mg L^{-1}, Table S1) the c_{H2O2} values obtained for [Lake]UV were one order of magnitude above those previously reported[50], which may account for the additive effect of c_{H2O2} on oxidative stress observed in *C. reinhardtii* in our experimental setup.

In MOPS, abiotic c_{H2O2} were higher in UV treatments but all other trends by and large remained the same as in the non-UV treatment.

CONCLUSION

This is the first in-depth nano-ecotoxicological study to continuously quantify abiotic and biotic nano-TiO_2 – stimulated extracellular H_2O_2 during 1 h exposure of *C. reinhardtii*. It is also the first attempt to link extracellular H_2O_2 to standard nano-ecotoxicological endpoints of cellular pro-oxidant processes.

It was found that agglomerated nano-TiO_2 generated cellular pro-oxidant responses, which are significantly modified by the parameters exposure medium, exposure time, UV pre-illumination as well as exposure concentrations. Furthermore, extra- and intracellular pro-oxidant processes differed significantly: intracellular oxidative stress increased in conditions where no significant increase in extracellular H_2O_2 was measured and elevated extracellular levels of abiotic H_2O_2 did not point to intracellular oxidative stress.

Thus, nano-TiO_2 toxicity is not mediated by pro-oxidant processes alone and extracellular H_2O_2 cannot serve as a predictor of cellular oxidative stress and damage. These findings are important with respect to future ecotoxicological endeavors seeking to link physicochemical particle properties with exposure scenarios and biological responses for ENM hazard assessment and prediction.

ACKNOWLEDGEMENTS

This work was part of the National Research Program 64 on the Opportunities and Risk of Nanomaterials with the project number 406440-131280, funded by the Swiss National Science Foundation. Many thanks are extended to Maurus Thurneysen for support in statistical analyses with R.

DECLARATION OF INTEREST

All authors declare that there are no conflicts of interest.

REFERENCES

1. T. M. Scown, R. van Aerle and C. R. Tyler, *Crit Rev Toxicol*, 2010, **40**, 653-670.
2. M. N. Moore, *Environ. Int.*, 2006, **32**, 967-976.
3. S. J. Klaine, A. A. Koelmans, N. Horne, S. Carley, R. D. Handy, L. Kapustka, B. Nowack and F. v. d. Kammer, *Environ. Toxicol. Chem.*, 2012, **31**, 3-14.
4. A. Bour, F. Mouchet, J. Silvestre, L. Gauthier and E. Pinelli, *J Hazard Mater*, 2015, **283**, 764-777.
5. A. B. Djurisic, Y. H. Leung, A. M. C. Ng, X. Y. Xu, P. K. H. Lee, N. Degger and R. S. S. Wu, *Small*, 2015, **11**, 26-44.
6. N. von Moos, P. Bowen and V. I. Slaveykova, *Environmental Science: Nano*, 2014, **1**, 214-232.
7. E. Burello and A. P. Worth, *Nanotoxicology*, 2011, **5**, 228-235.
8. H. Zhang, Z. Ji, T. Xia, H. Meng, C. Low-Kam, R. Liu, S. Pokhrel, S. Lin, X. Wang, Y.-P. Liao, M. Wang, L. Li, R. Rallo, R. Damoiseaux, D. Telesca, L. Mädler, Y. Cohen, J. I. Zink and A. E. Nel, *ACS Nano*, 2012, **6**, 4349-4368.
9. A. Nel, T. Xia, L. Madler and N. Li, *Science*, 2006, **311**, 622-627.
10. A. E. Nel, L. Mädler, D. Velegol, T. Xia, E. M. V. Hoek, P. Somasundaran, F. Klaessig, V. Castranova and M. Thompson, *Nat. Mater.*, 2009, **8**, 543-557.
11. A. L. Neal, *Ecotoxicology*, 2008, **17**, 362-371.
12. T. Xia, M. Kovochich, J. Brant, M. Hotze, J. Sempf, T. Oberley, C. Sioutas, J. I. Yeh, M. R. Wiesner and A. E. Nel, *Nano Lett*, 2006, **6**, 1794-1807.
13. K. Donaldson, P. H. Beswick and P. S. Gilmour, *Toxicol Lett*, 1996, **88**, 293-298.
14. S. J. Soenen, P. Rivera-Gil, J.-M. Montenegro, W. J. Parak, S. C. De Smedt and K. Braeckmans, *Nano Today*, 2011, **6**, 446-465.
15. N. von Moos and V. Slaveykova, *Nanotoxicology*, 2013, **8**, 605-630.
16. D. R. Livingstone, *Mar Pollut Bull*, 2001, **42**, 656-666.
17. B. Halliwell and J. M. C. Gutteridge, eds., *Free radicals in biology and medecine*, Oxford University Press Inc, 2007.
18. M. Dynowski, G. Schaaf, D. Loque, O. Moran and U. Ludewig, *Biochemical Journal*, 2008, **414**, 53-61.
19. G. P. Bienert, A. L. B. Moller, K. A. Kristiansen, A. Schulz, I. M. Moller, J. K. Schjoerring and T. P. Jahn, *J Biol Chem*, 2007, **282**, 1183-1192.
20. V. Demidchik, *Environmental and Experimental Botany*, 2015, **109**, 212-228.
21. K. Aschberger, C. Micheletti, B. Sokull-Kluttgen and F. M. Christensen, *Environ. Int.*, 2011, **37**, 1143-1156.
22. M. A. Torres, M. P. Barros, S. C. G. Campos, E. Pinto, S. Rajamani, R. T. Sayre and P. Colepicolo, *Ecotox Environ Safe*, 2008, **71**, 1-15.
23. B. Fadeel and A. E. Garcia-Bennett, *Adv Drug Deliver Rev*, 2010, **62**, 362-374.
24. A. Weir, P. Westerhoff, L. Fabricius, K. Hristovski and N. von Goetz, *Environ Sci Technol*, 2012, **46**, 2242-2250.
25. Y. Yang, K. Doudrick, X. Y. Bi, K. Hristovski, P. Herckes, P. Westerhoff and R. Kaegi, *Environ Sci Technol*, 2014, **48**, 6391-6400.
26. X. Chen and S. S. Mao, *Chem Rev*, 2007, **107**, 2891-2959.

27. O. Carp, C. L. Huisman and A. Reller, *Prog Solid State Ch*, 2004, **32**, 33-177.
28. R. X. Cai, Y. Kubota, T. Shuin, H. Sakai, K. Hashimoto and A. Fujishima, *Cancer Research*, 1992, **52**, 2346-2348.
29. R. Cai, K. Hashimoto, Y. Kubota and A. Fujishima, *Chemistry Letters*, 1992, DOI: 10.1246/cl.1992.427, 427-430.
30. H. A. Foster, I. B. Ditta, S. Varghese and A. Steele, *Appl Microbiol Biot*, 2011, **90**, 1847-1868.
31. F. Hossain, O. J. Perales-Perez, S. Hwang and F. Román, *Sci Total Environ*, 2014, **466–467**, 1047-1059.
32. B. Salieri, S. Righi, A. Pasteris and S. I. Olsen, *Sci Total Environ*, 2015, **505**, 494-502.
33. C. A. Linkous, G. J. Carter, D. B. Locuson, A. J. Ouellette, D. K. Slattery and L. A. Smitha, *Environ Sci Technol*, 2000, **34**, 4754-4758.
34. W.-M. Lee and Y.-J. An, *Chemosphere*, 2013, **91**, 536-544.
35. K. Hund-Rinke and M. Simon, *Environ Sci Pollut R*, 2006, **13**, 225-232.
36. J. X. Wang, X. Z. Zhang, Y. S. Chen, M. Sommerfeld and Q. Hu, *Chemosphere*, 2008, **73**, 1121-1128.
37. F. M. Li, Z. Liang, X. Zheng, W. Zhao, M. Wu and Z. Y. Wang, *Aquat Toxicol*, 2015, **158**, 1-13.
38. E. H. Harris, *The Chlamydomonas Sourcebook - a Comprehensive Guide to Biology and Laboratory Use*, Academic Press, San Diego CA, 2nd edn., 2009.
39. M. Senna, N. Myers, A. Aimable, V. Laporte, C. Pulgarin, O. Baghriche and P. Bowen, *Journal of Materials Research*, 2013, **28**, 354-361.
40. P. J. Neale, P. Bossard and Y. Huot, *Aquat Sci*, 2001, **63**, 250-264.
41. A. Ivask, T. Titma, M. Visnapuu, H. Vija, A. Kakinen, M. Sihtmae, S. Pokhrel, L. Madler, M. Heinlaan, V. Kisand, R. Shimmo and A. Kahru, 2015, **15**, 1914-1929.
42. J. H. Priester, P. K. Stoimenov, R. E. Mielke, S. M. Webb, C. Ehrhardt, J. P. Zhang, G. D. Stucky and P. A. Holden, *Environ Sci Technol*, 2009, **43**, 2589-2594.
43. V. B. Koman, C. Santschi, N. R. von Moos, V. I. Slaveykova and O. J. F. Martin, *Biosensors and Bioelectronics*, 2015, **68**, 245-252.
44. N. von Moos, L. Maillard and V. I. Slaveykova, *Aquat Toxicol*, 2015, **161**, 267-275.
45. P. Baveye and M. Laba, *Environ Health Persp*, 2008, **116**, A152-A152.
46. C. Perstrimaux, S. Le Faucheur, M. Mortimer, S. Stoll, F. B. Aubry, M. Botter, R. Zonta and V. I. Slaveykova, *Aquatic Geochemistry*, 2014, 1-20.
47. A. A. Keller, H. T. Wang, D. X. Zhou, H. S. Lenihan, G. Cherr, B. J. Cardinale, R. Miller and Z. X. Ji, *Environ. Sci. Technol.*, 2010, **44**, 1962-1967.
48. F. Loosli, P. Le Coustumer and S. Stoll, *Water Res.*, 2013, **47**, 6052-6063.
49. J. M. Burns, W. J. Cooper, J. L. Ferry, D. W. King, B. P. DiMento, K. McNeill, C. J. Miller, W. L. Miller, B. M. Peake, S. A. Rusak, A. L. Rose and T. D. Waite, *Aquat Sci*, 2012, **74**, 683-734.
50. F. Leunert, W. Eckert, A. Paul, V. Gerhardt and H.-P. Grossart, *J Plankton Res*, 2014, **36**, 185-197.
51. M. Cho, H. Chung, W. Choi and J. Yoon, *Water Res*, 2004, **38**, 1069-1077.
52. S. P. Yang, O. Bar-Ilan, R. E. Peterson, W. Heideman, R. J. Hamers and J. A. Pedersen, *Environ Sci Technol*, 2013, **47**, 4718-4725.
53. D. Lin, J. Ji, Z. Long, K. Yang and F. Wu, *Water Res*, 2012, **46**, 4477-4487.
54. R. Kohen and A. Nyska, *Toxicol Pathol*, 2002, **30**, 620-650.
55. I. Szivak, R. Behra and L. Sigg, *J Phycol*, 2009, **45**, 427-435.
56. D. M. Metzler, M. Li, A. Erdem and C. P. Huang, *Chemical Engineering Journal*, 2011, **170**, 538-546.
57. I. M. Sadiq, S. Dalai, N. Chandrasekaran and A. Mukherjee, *Ecotox Environ Safe*, 2011, **74**, 1180-1187.
58. J. Ji, Z. Long and D. Lin, *Chem. Eng. J.*, 2011, **170**, 525-530.

59. O. K. Dalrymple, E. Stefanakos, M. A. Trotz and D. Y. Goswami, *Appl Catal B-Environ*, 2010, **98**, 27-38.
60. P. C. Maness, S. Smolinski, D. M. Blake, Z. Huang, E. J. Wolfrum and W. A. Jacoby, *Appl Environ Microb*, 1999, **65**, 4094-4098.
61. H. E. Zagarese and C. E. Williamson, *Fish and Fisheries*, 2001, **2**, 250-260.
62. M. I. Gonzalez-Sanchez, L. Gonzalez-Macia, M. T. Perez-Prior, E. Valero, J. Hancock and A. J. Killard, *Plant Cell Environ*, 2013, **36**, 869-878.
63. A. Levine, R. Tenhaken, R. Dixon and C. Lamb, *Cell*, 1994, **79**, 583-593.